

SULFUR MOLECULE CHEMISTRY IN SUPERNOVA EJECTA RECORDED BY SILICON CARBIDE STARDUST

PETER HOPPE¹, WATARU FUJIYA², AND ERNST ZINNER³

¹ Max Planck Institute for Chemistry, Hahn-Meitner-Weg 1, 55128 Mainz, Germany; peter.hoppe@mpic.de

² Department of Earth and Planetary Science, University of Tokyo, 7-3-1 Hongo, Bunkyo-ku, Tokyo 113-0033, Japan; fujiya@eps.s.u-tokyo.ac.jp

³ Laboratory for Space Sciences and Physics Department, Campus Box 1105, Washington University, St. Louis, MO 63130, USA; ekz@wustl.edu

Received 2011 November 7; accepted 2011 December 19; published 2012 January 11

ABSTRACT

We studied about 3400 presolar silicon carbide (SiC) grains from the Murchison CM2 meteorite for C- and Si-isotopic compositions. Among these grains we identified 7 unusual or type C SiC (U/C) grains, characterized by isotopically heavy Si, and 36 supernova type X SiC grains, characterized by isotopically light Si. Selected U/C and X grains were also measured for S-, Mg–Al-, and Ca–Ti-isotopic compositions. We show that the U/C grains incorporated radioactive ⁴⁴Ti, which is evidence that they formed in the ejecta of Type II supernova (SNII) explosions. Abundances of radioactive ²⁶Al and ⁴⁴Ti are compatible with those observed in X grains. U/C and X grains carry light S with enrichments in ³²S of up to a factor of 2.7. The combination of heavy Si and light S observed in U/C grains is not consistent with abundance predictions of simple supernova models. The isotope data suggest preferential trapping of S from the innermost supernova zones, the production site of radioactive ⁴⁴Ti, by the growing silicon carbide particles. A way to achieve this is by sulfur molecule chemistry in the still unmixed ejecta. This confirms model predictions of molecule formation in SNII ejecta and shows that sulfur molecule chemistry operates in the harsh and hot environments of stellar explosions.

Key words: circumstellar matter – molecular processes – nuclear reactions, nucleosynthesis, abundances – supernovae: general

Online-only material: color figures

1. INTRODUCTION

Sulfur is the tenth most abundant element in the cosmos (Lodders 2003). It has four stable isotopes, ³²S, ³³S, ³⁴S, and ³⁶S with abundances of 95%, 0.75%, 4.2%, and 0.015%, respectively, which are produced mainly in massive stars and expelled into the interstellar medium (ISM) when these stars explode, e.g., as Type II supernovae (SNeII; Timmes et al. 1995). Sulfur forms a variety of molecules that are important for many chemical and physical processes in diverse environments. Sulfur-bearing molecules are observed in the ISM (Tielens 2005) and around low- and intermediate-mass stars, e.g., the carbon star IRC + 10216 (Kahane et al. 1988). A large amount of S molecules are also predicted by models of molecule formation in Type II supernova (SNII) ejecta (Cherchneff & Dwek 2009). In this work, we give the first observational evidence, based on the study of so-called presolar grains, that the S molecule formation takes place in the harsh, hot (temperatures of several 1000 K) environment of stellar explosions.

Presolar grains are samples of stardust that are found in small quantities in primitive solar system materials, such as meteorites, interplanetary dust particles, and cometary matter (Zinner 2007). They formed in the winds of evolved stars or in the ejecta of stellar explosions. After passing through the ISM they became part of the gas and dust cloud from which our solar system formed some 4.6 Gyr ago and survived all stages of solar system formation. Laboratory studies of presolar grains provide detailed insights into physical and chemical processes in stellar environments. Presolar grains exhibit large isotopic anomalies in the major and minor elements, preserving the nucleosynthetic signature of their parent stars. Among the identified presolar minerals is silicon carbide (SiC). It is well established that most presolar SiC grains formed in the winds of 1–3 M_{\odot} asymptotic giant branch stars (Lugaro et al. 2003). The so-called X grains, which constitute about 1% of the presolar SiC

grains, originate from the ejecta of supernova (SN) explosions. They are characterized by higher than solar ¹²C/¹³C (most grains) and lower than solar ¹⁴N/¹⁵N and ^{29,30}Si/²⁸Si ratios, and they show large excesses in ²⁶Mg, ⁴⁴Ca, and ⁴⁹Ti due to the decay of radioactive ²⁶Al (half-life 716,000 yr), ⁴⁴Ti (half-life 60.4 yr), and, at least in part, ⁴⁹V (half-life 330 days; Amari et al. 1992; Nittler et al. 1996; Hoppe et al. 2000; Hoppe & Besmehn 2002; Besmehn & Hoppe 2003; Lin et al. 2010). Specifically, diagnostic for the SN origin of X grains are large excesses in ²⁸Si, very high initial ²⁶Al/²⁷Al ratios of 0.01–0.6, and the presence of now extinct ⁴⁴Ti with initial ⁴⁴Ti/⁴⁸Ti ratios between 10^{−3} and 1. Although certain problems exist, many isotopic signatures of X grains can be well reproduced by so-called ad hoc SNII mixing models. In this approach, matter from different SNII zones is mixed in variable proportions, with the proportions of different elements from a given zone remaining the same, i.e., no elemental fractionation is assumed (e.g., Travaglio et al. 1999; Hoppe et al. 2000).

An SNII origin has also been proposed for SiC grains with isotopically heavy Si (excesses in ²⁹Si of more than 25%; Amari et al. 1999; Croat et al. 2010; Gyngard et al. 2010a; Hoppe et al. 2010; Zinner et al. 2010). These rare grains have been named “unusual” (Hoppe et al. 2010) or “Type C” (Gyngard et al. 2010a; in the following designated as U/C grains) and are found predominantly among the smallest, i.e., submicrometer-sized, grains. Like X grains, they have higher than solar ¹²C/¹³C (most grains) and lower than solar ¹⁴N/¹⁵N ratios. Two of them were shown to carry large enrichments in ³²S (Gyngard et al. 2010a; Hoppe et al. 2010). Their C-, N-, Si-, and S-isotopic signatures point toward an SNII origin. However, the presence of heavy Si together with light S in SNII grains poses a fundamental problem. Silicon- and S-isotopic signatures (isotopically heavy or light) are the same in the different SNII zones (Figure 1; Rauscher et al. 2002) and ad hoc mixing scenarios that reproduce the heavy Si in U/C grains predict heavy S as well. Thus, the

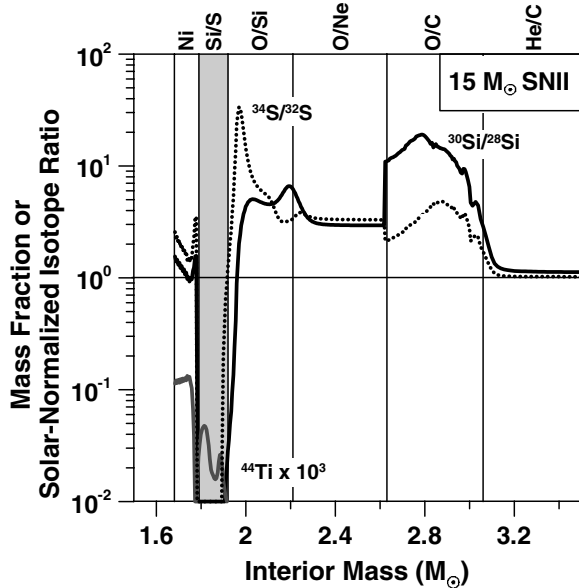


Figure 1. Model predictions of solar-normalized $^{30}\text{Si}/^{28}\text{Si}$ and $^{34}\text{S}/^{32}\text{S}$ ratios as well as the ^{44}Ti mass fraction (multiplied by 10^3) in the interior of a $15 M_{\odot}$ SNII (Rauscher et al. 2002). The eight SN zones are designated at the top of the figure. Qualitatively, S and Si isotope signatures (i.e., light/heavy) are the same in the different SN zones. The only zone that has light Si and S is the Si/S zone (marked in gray). Titanium-44 is produced only in the interior Ni and Si/S zones.

combination of heavy Si with light S in U/C grains cannot be explained by simple ad hoc mixing models based on the SNeII considered here (i.e., mixing without any element fractionation of material from a given zone).

Here we present results of comprehensive isotope studies on new X and U/C grains aimed at (1) obtaining a definitive proof of the proposed SN origin of U/C grains and (2) understanding the S-isotopic signature of SN dust and its importance for chemical and physical processes in SNII ejecta.

2. EXPERIMENTAL PROCEDURES

The SiC grains of this study were separated from a 30 g sample of the Murchison CM2 meteorite (Besmehn & Hoppe 2003), following the technique described by Amari et al. (1994). Thousands of SiC grains were deposited from liquid suspension onto several clean Au foils, one of which (sample “Muri7,” abbreviated here as “M7”) was used for the present study. Areas suitable for ion imaging (see below) were selected in the Leo 1530 field emission SEM at the Max Planck Institute for Chemistry in Mainz.

The search for SiC grains with large excesses in the heavy Si isotopes was done by ion imaging with the Cameca NanoSIMS 50 ion probes at Max Planck Institute for Chemistry (Gröner & Hoppe 2006) and Washington University (Gyngard et al. 2010b). Prior to ion imaging the analyzed areas were cleaned and implanted with Cs for several minutes by pre-sputtering with a high-current Cs^+ ion beam. The application of ion imaging to SiC grain mounts consists essentially of three steps: (1) acquisition of ion images of $^{12}\text{C}^-$, $^{13}\text{C}^-$, $^{28}\text{Si}^-$, $^{29}\text{Si}^-$, and $^{30}\text{Si}^-$ in a multi-collection mode, produced by rastering (256×256 pixels, $5000\text{--}15,000 \mu\text{s pixel}^{-1}$) a focused primary Cs^+ ion beam (~ 100 nm, ~ 1 pA) over 30×30 (MPI) or 20×20 (WU) μm^2 sized areas on the Au foil. (2) Identification of SiC grains based on the ^{28}Si ion image. Acquisition of ion images with sizes of two times the grain size around each identified

grain with an integration time of 60 s (MPI), or measurements of individual SiC grains in the so-called NanoSIMS grain mode (integration of ion intensities) with integration times adjusted according to grain size (WU). (3) Movement of the sample stage to an adjacent area and repetition of steps (1)–(3). A total of 99 (MZ) and, respectively, 464 (WU) areas were analyzed in this way on which ~ 3400 presolar SiC grains were measured. Among these grains we identified 7 U/C grains and 36 X grains.

Five U/C grains and twenty-two X grains were subsequently re-analyzed for C- and Si-isotopic compositions by acquiring high-resolution images ($3 \times 3 \mu\text{m}^2$, 128×128 pixels, $10,000 \mu\text{s pixel}^{-1}$, otherwise the same setup as for automated ion imaging) to exclude contributions from other attached or nearby SiC grains to the C and Si ion signals from the selected grains. Sulfur-isotopic compositions were measured on these 27 grains by recording $^{28}\text{Si}^-$, $^{32}\text{S}^-$, $^{33}\text{S}^-$, and $^{34}\text{S}^-$ ions with a similar analysis setup as for the high-resolution C and Si imaging ($1.5\text{--}3 \times 1.5\text{--}3 \mu\text{m}^2$, 128×128 or 256×256 pixels, $3000\text{--}10,000 \mu\text{s pixel}^{-1}$, 2–17 image planes). In addition, we measured Mg–Al- and Ca–Ti-isotopic compositions in the two largest U/C grains. These measurements were performed by rastering (256×256 pixels, $10,000 \mu\text{s pixel}^{-1}$, 2–3 image planes) an O^- primary ion beam (~ 5 pA, 300–400 nm) over $3\text{--}5 \times 3\text{--}5 \mu\text{m}^2$ sized areas around the grains. For Ca–Ti positive secondary ions of ^{28}Si , ^{40}Ca , ^{42}Ca , and ^{44}Ca , and ^{48}Ti were measured in a multi-collection mode, and for Mg–Al ^{24}Mg , ^{25}Mg , ^{26}Mg , ^{27}Al , and ^{28}Si .

Instrumental mass fractionation and variations in the detection efficiencies of the different electron multipliers for the isotope measurements were corrected by measurements on synthetic, fine-grained SiC (C, Si, and also S, which is present in sufficiently high quantities), S-rich material (contamination) on the M7 mount, Burma spinel (Mg–Al), and perovskite (Ca–Ti). The relative sensitivity factor $\varepsilon(\text{Al}^+)/\varepsilon(\text{Mg}^+) = 1.56$, needed to infer initial $^{26}\text{Al}/^{27}\text{Al}$ ratios, was taken from Hoppe et al. (2010) and $\varepsilon(\text{Ti}^+)/\varepsilon(\text{Ca}^+) = 0.51$, needed to infer the initial $^{44}\text{Ti}/^{48}\text{Ti}$ ratios, was taken from Besmehn & Hoppe (2003). Trace element abundances given in Table 1 have been calculated with the sensitivity factors $\varepsilon(\text{Al}^+)/\varepsilon(\text{Si}^+) = 4.0$ (Hoppe et al. 2010), $\varepsilon(\text{Ti}^+)/\varepsilon(\text{Si}^+) = 4.2$ (Besmehn & Hoppe 2003), and $\varepsilon(\text{S}^-)/\varepsilon(\text{Si}^-) = 3$; the latter was estimated from measurements of Si and S ion yields on synthetic SiC and Mundrabilla FeS, respectively.

3. RESULTS AND DISCUSSION

The isotope data of the five U/C grains (M7-A...E) and of one X grain (M7-X18) are given in Table 1. Silicon isotope data of the five U/C grains and of seven X grains that have errors of less than 150‰ in $\delta^{33}\text{S}$ (see below) are displayed in Figure 2. All U/C grains exhibit overabundances in ^{32}S (or corresponding depletions in $^{33,34}\text{S}$), especially grains M7-C and M7-D, which show depletions in the $^{33}\text{S}/^{32}\text{S}$ and $^{34}\text{S}/^{32}\text{S}$ ratios of more than a factor of two (Figure 3). Contamination by S on or in very close proximity of individual SiC grains complicated these measurements and the data of grains M7-A, M7-B, and M7-E are likely to be affected by contributions of terrestrial S, i.e., intrinsic S-isotopic anomalies might be more extreme. The problem of S contamination turned out to be even more severe for X grains. For six X grains the S signal was clearly dominated by contamination, as evidenced from the spatial distribution of S and Si in the ion images. For the remaining 16 X grains the problem was less severe, though still present. Nevertheless, in

Table 1
Isotopic Compositions and Trace Element Abundances of SiC SN Grains from the Murchison Meteorite

Grain	Size (μm)	$^{12}\text{C}/^{13}\text{C}$	$\delta^{29}\text{Si}$ (‰)	$\delta^{30}\text{Si}$ (‰)	$\delta^{33}\text{S}$ (‰)	$\delta^{34}\text{S}$ (‰)	[S] (wt%)
M7-A	0.5	59 ± 3	996 ± 37	1010 ± 46	-72 ± 130	-115 ± 55	0.77
M7-B	0.3	178 ± 20	1149 ± 70	826 ± 79	-284 ± 207	7 ± 106	1.60
M7-C	0.7	152 ± 5	800 ± 15	1367 ± 21	-624 ± 84	-642 ± 35	0.15
M7-D	1.0	109 ± 2	1082 ± 12	1207 ± 16	-609 ± 61	-478 ± 142	0.17
M7-E	0.4	1.304 ± 0.004	313 ± 7	377 ± 9	-227 ± 161	-96 ± 74	0.27
M7-X18	0.5	131 ± 2	-199 ± 5	-317 ± 6	-356 ± 114	-209 ± 53	0.11
		$^{26}\text{Al}/^{27}\text{Al}$	[Al] (wt%)	$\delta^{42}\text{Ca}$ (‰)	$\delta^{44}\text{Ca}$ (‰)	$^{44}\text{Ti}/^{48}\text{Ti}$	[Ti] (wt%)
M7-A							
M7-B							
M7-C		0.015 ± 0.004	3.3	-213 ± 280	1854 ± 307	0.013 ± 0.002	0.48
M7-D		0.122 ± 0.012	1.1	-142 ± 240	18160 ± 530	0.077 ± 0.002	0.11
M7-E							
M7-X18							

Note. $\delta^xE = [(^xE/^{\text{ref}E})_{\text{Grain}} / (^xE/^{\text{ref}E})_{\odot} - 1] \times 1000$; $\text{ref}E = ^{28}\text{Si}$, ^{32}S , or ^{40}Ca .

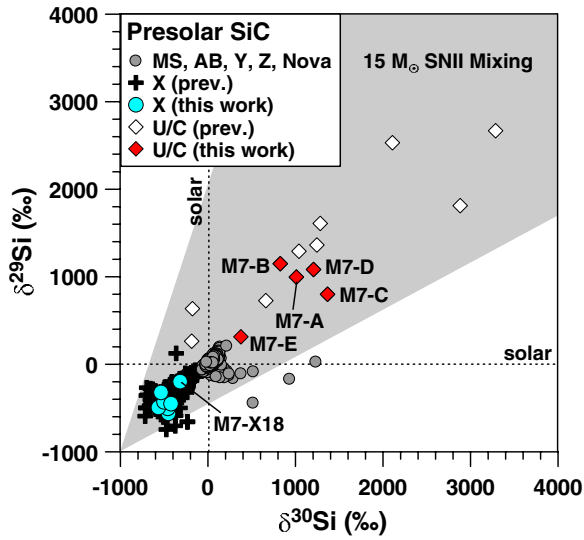


Figure 2. Si-isotopic compositions of different types of presolar SiC grains. For a definition of grain types see Zinner (2007). The grains studied in this work (Murchison sample M7) are marked in blue (X grains; only the seven X grains displayed in Figure 3 are shown) and in red (U/C grains; two U/C grains sputtered away during ion imaging and are not shown). The range of possible Si-isotopic compositions, which result from the mixing of matter from different zones in a $15 M_{\odot}$ SNII (Rauscher et al. 2002), is shown in gray. (A color version of this figure is available in the online journal.)

one case (M7-X18) a clear excess in ^{32}S was seen and also most of the remaining grains tend to have isotopically light S: even if grain M7-X18 is excluded, mass-weighted averages of $^{33}\text{S}/^{32}\text{S}$ and $^{34}\text{S}/^{32}\text{S}$ in the remaining 15 X grains show anomalies of $>2\sigma$ (Figure 3). Magnesium in U/C grains M7-C and M7-D is essentially monoisotopic ^{26}Mg , clear evidence for ^{26}Al decay. The inferred initial $^{26}\text{Al}/^{27}\text{Al}$ ratios of 0.015 and 0.12 are in the range of typical X grains (Figure 4). Both grains have close-to-solar $^{42}\text{Ca}/^{40}\text{Ca}$ ratios but large excesses in $^{44}\text{Ca}/^{40}\text{Ca}$ of up to a factor of ~ 20 . This signature can be explained only if decay of radioactive ^{44}Ti is invoked. The inferred initial $^{44}\text{Ti}/^{48}\text{Ti}$ ratios of ~ 0.01 and ~ 0.08 are well within the range of X grains (Figure 4). The detection of now extinct ^{44}Ti , which can be produced only in SN explosions (Woosley et al. 1973; Timmes et al. 1996), is definitive proof of

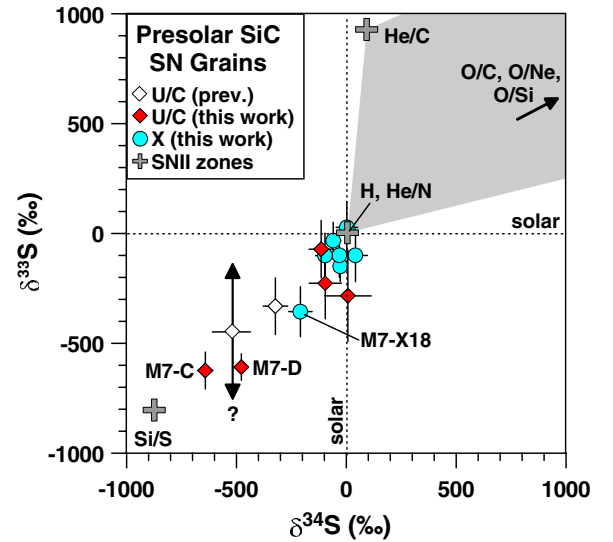


Figure 3. Sulfur-isotopic compositions of SiC SN grains. X grain data are only shown if the error in $\delta^{33}\text{S}$ is less than 150%. The question mark indicates that no $^{33}\text{S}/^{32}\text{S}$ ratio is available. For three grains from this study (M7-C, M7-D, M7-X18) clear depletions in ^{33}S and ^{34}S are seen. The predicted S-isotopic compositions of the different zones in a $15 M_{\odot}$ SNII (Rauscher et al. 2002) are shown as gray crosses, and mixtures of O- and C-rich layers as gray-shaded region.

(A color version of this figure is available in the online journal.)

the SNII origin of U/C grains. This is in line with conclusions previously drawn for SiC X and SN graphite grains (Hoppe et al. 1996; Nittler et al. 1996) and an SN spinel grain (Gyngard et al. 2010b).

About one-third of sub-micrometer-sized X grains (Hoppe et al. 2010) as well as two of the U/C grains from this study show isotopic enrichments in ^{13}C , i.e., $^{12}\text{C}/^{13}\text{C}$ ratios lower than the solar ratio of 89. Heavy C can be explained by ad hoc SNII mixing models if comparatively large contributions from the outer He/N and H zones are considered. U/C grain M7-E has a particularly low $^{12}\text{C}/^{13}\text{C}$ ratio and its $^{12}\text{C}/^{13}\text{C}$ ratio of 1.3 is lower than the lowest achievable $^{12}\text{C}/^{13}\text{C}$ of ~ 3 in the He/N and Ni zones of SNII models (Rauscher et al. 2002). A possible mechanism to account for very low $^{12}\text{C}/^{13}\text{C}$ ratios

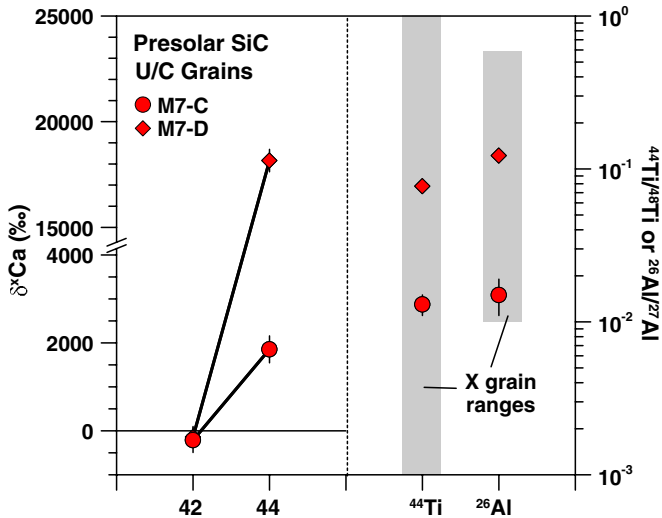


Figure 4. Left panel: calcium-isotopic compositions of SiC U/C grains M7-C and M7-D. The large excesses in ^{44}Ca along with close-to-normal $^{42}\text{Ca}/^{40}\text{Ca}$ ratios are indicative of ^{44}Ti decay. Right panel: inferred $^{44}\text{Ti}/^{48}\text{Ti}$ and $^{26}\text{Al}/^{27}\text{Al}$ ratios of grains M7-C and M7-D and, in gray, the observed ranges for SN X grains.

(A color version of this figure is available in the online journal.)

in certain SNI zones may be rotational mixing. The effect of rotation on the production of C and N isotopes in pre-SN stars was explored by Langer et al. (1998). These authors found that rotational-induced mixing may produce a ^{13}C -rich layer just below the H-burning shell (He/N zone). As pointed out by Nittler & Hoppe (2005), a contribution from this ^{13}C -rich layer to the SiC condensation site in the SNI ejecta provides a plausible explanation for SNI grains with very low $^{12}\text{C}/^{13}\text{C}$ ratios. However, the currently available one-dimensional stellar models including rotation still have serious limitations and it remains to be seen whether the results from improved, multi-dimensional models will lead to similar conclusions.

The finding of now extinct ^{44}Ti in U/C grains shows that these grains incorporated matter from the Si/S and possibly Ni zone. The measured C- and Si-isotopic compositions as well as the $^{26}\text{Al}/^{27}\text{Al}$ and $^{44}\text{Ti}/^{48}\text{Ti}$ ratios of grains M7-C and M7-D can be very well matched by ad hoc mixing of layers predicted by the $15 M_{\odot}$ SNI model of Rauscher et al. (2002), with most matter coming from the outer H- and He-rich zones (He/C, He/N, H; total contribution 96%–97%) and small contributions from the intermediate O-rich (3%–4%) and the inner Ni/Si/S-rich zones (0.1%–0.2%). However, the S-isotopic ratios cannot be reproduced by these mixing scenarios and predicted $^{34}\text{S}/^{32}\text{S}$ ratios are by factors of 5–6 too high. A similar conclusion is derived from the solar-metallicity $25 M_{\odot}$ SNI model of Rauscher et al. (2002). Nevertheless, we note that SNI models are still afflicted with large uncertainties concerning the yields of specific nuclides, e.g., due to the interaction between the internal shells before core collapse (Arnett & Meakin 2011) or due to the effect of neutrino-driven winds on SNI nucleosynthesis (Roberts et al. 2010). In the context of the $15 M_{\odot}$ SNI model of Rauscher et al. (2002) considered here the only plausible solution to the S problem of the U/C grains is fractionation between Si and S in the contributions from different SNI zones. We propose that in order to account for the observed S-isotopic compositions of grains M7-C and M7-D, S from the Si/S zone was captured by the growing SiC grains about 40–50× more efficiently than S from the other zones.

A way to achieve this is by molecule chemistry in SNI ejecta. Molecules such as CO and SiO have been observed in the ejecta of SN1987A (Wooden et al. 1993). Molecules are important for the pathways of dust formation and the dissociation of CO by energetic electrons produced by radioactivity has been considered to be a key factor for the growth of carbon particles in SNI ejecta (Clayton et al. 1999). According to models of chemical kinetics in SNI from zero-metallicity progenitor stars, a large amount of molecules are expected to form in the ejecta (Cherchneff & Dwek 2009). The amount and the molecule species depend sensitively on the mass and metallicity of the progenitor star, the SNI nucleosynthesis model used as an input, and the degree of mixing. In any case, S molecules are predicted to be important constituents of the ejecta. For a $20 M_{\odot}$ SNI (zero-metallicity progenitor) without mixing, about 7% of all matter is predicted to be in the molecular form (Cherchneff & Dwek 2009). The most abundant species are SiS, which forms efficiently in ejecta from the Ni/Si/S zone, and O_2 , CO, and SO from the O-rich zones. One thousand days after explosion, SiS is predicted to make up about 1% of all ejected matter. It starts forming efficiently after ~ 200 days (when temperatures dropped to ~ 5000 K). It is absent in material from the zones on top of the Ni/Si/S core. Sulfur monoxide, on the other hand, starts to form in significant amounts, although less abundant than SiS from the Ni/Si/S zone, in the O-rich ejecta after ~ 350 days (Cherchneff & Dwek 2009). Our data suggest that molecule formation occurs in largely unmixed ejecta, followed by macroscopic mixing (e.g., due to Rayleigh–Taylor instabilities; Kifonidis et al. 2003) and finally the growth of SiC particles. Under equilibrium conditions, SiS plays an important role in the formation of SiC (Lodders & Fegley 1995). It is thus conceivable that S is captured by the growing SiC particles as SiS while uptake of S from other zones, either bound in SO or as elemental S, is strongly suppressed. At the same time, Si is incorporated from other zones as well. Because X grains are ^{28}Si -rich (Figure 2), which suggests a stronger contribution from the Si/S zone compared to U/C grains, one would expect to find even larger ^{32}S enrichments in X than in U/C grains. However, X grains show milder ^{32}S enrichments than U/C grains (Figure 3). As we have pointed out, S contamination is a serious and unavoidable problem which might have lowered intrinsic S isotope anomalies to varying degrees. Indeed, it is possible that in X grains the invoked S fractionation for U/C grains is smaller and intrinsic S concentrations lower. Therefore, the finding of ^{32}S enrichments in X grains in addition to U/C grains lends strong support to the conclusion that U/C grains have preserved a record of S molecule chemistry in their parent SNI ejecta.

Sulfur molecule chemistry in SNI ejecta may also offer a solution for the yet unexplained Fe isotope signatures of X grains (Marhas et al. 2008). Similar to Si and S in U/C grains it is not possible to account for the combination of observed Si- and Fe-isotopic compositions in X grains by ad hoc SNI mixing. Iron in X grains is characterized by solar $^{54}\text{Fe}/^{56}\text{Fe}$ and higher than solar $^{57}\text{Fe}/^{56}\text{Fe}$ ratios. The light Si of X grains requires significant contributions from the Si/S zone, which should lead to higher than solar $^{54}\text{Fe}/^{56}\text{Fe}$ ratios, contrary to the observation. The Fe-isotopic signature of X grains can be explained by preferential trapping of Fe from the He/C and He/N zones over Fe from the Si/S zone. A fractionation factor of >10 is required to account for the observed Fe-isotopic signatures. By forming FeS dust or FeS molecule cluster in ejecta from the Ni/Si/S zone it might be possible to largely prevent Fe from the Si/S zone to be trapped by the growing SiC

grains. This idea is supported by models of molecule and dust chemistry in SNII ejecta that predict formation of significant amounts of FeS molecule clusters, the precursors of FeS dust, in the inner Ni/Si/S zone of unmixed SNII ejecta (Cherchneff & Dwek 2010). While in the zero-metallicity progenitor $20 M_{\odot}$ star considered by Cherchneff & Dwek (2010), 44% of Fe from the Ni/Si/S zone is predicted to be in $(\text{FeS})_4$ clusters, this fraction reaches 80% in models of molecule formation based on the solar-metallicity 15, 20, and $25 M_{\odot}$ SNII models of Rauscher et al. (2002) (I. Cherchneff 2011, private communication). Such large fraction of $(\text{FeS})_4$ clusters could provide a valuable scenario to explain the Fe isotope data of X grains.

We thank Joachim Huth for the SEM analyses, Elmar Gröner and Frank Gyngard for developing automatic grain mode programs, Tim Smolar for technical support on the NanoSIMS, Yuchen Xu for help during ion imaging, Isabelle Cherchneff for sharing unpublished data, and Alexander Heger for providing detailed SNII data on www.nucleosynthesis.org. Constructive comments by an anonymous reviewer helped to improve this manuscript. P.H. thanks Ramanath Cowsik for his hospitality at the McDonnell Center for the Space Sciences at Washington University. W.F. acknowledges support from the JSPS Global COE program of Tokyo Institute of Technology and the University of Tokyo, and E.Z. support from NASA's cosmochemistry program.

REFERENCES

- Amari, S., Hoppe, P., Zinner, E., & Lewis, R. S. 1992, *ApJ*, 394, L43
 Amari, S., Lewis, R. S., & Anders, E. 1994, *Geochim. Cosmochim. Acta*, 58, 459
 Amari, S., Zinner, E., & Lewis, R. S. 1999, *ApJ*, 517, L59
 Arnett, W. D., & Meakin, C. 2011, *ApJ*, 741, 33
 Besmehn, A., & Hoppe, P. 2003, *Geochim. Cosmochim. Acta*, 67, 4693
 Cherchneff, I., & Dwek, E. 2009, *ApJ*, 703, 642
 Cherchneff, I., & Dwek, E. 2010, *ApJ*, 713, 1
 Clayton, D. D., Liu, W., & Dalgarno, A. 1999, *Science*, 283, 1290
 Croat, T. K., Stadermann, F. J., & Bernatowicz, T. J. 2010, *AJ*, 139, 2159
 Gröner, E., & Hoppe, P. 2006, *Appl. Surf. Sci.*, 252, 7148
 Gyngard, F., Nittler, L. R., & Zinner, E. 2010a, *Meteorit. Planet. Sci.*, 45, A72
 Gyngard, F., Zinner, E., Nittler, L. R., et al. 2010b, *ApJ*, 717, 107
 Hoppe, P., & Besmehn, A. 2002, *ApJ*, 576, L69
 Hoppe, P., Leitner, J., Gröner, E., et al. 2010, *ApJ*, 719, 1370
 Hoppe, P., Strebel, R., Eberhardt, P., Amari, S., & Lewis, R. S. 1996, *Science*, 272, 1314
 Hoppe, P., Strebel, R., Eberhardt, P., Amari, S., & Lewis, R. S. 2000, *Meteorit. Planet. Sci.*, 35, 1157
 Kahane, C., Gomez-Gonzalez, J., Cernicharo, J., & Geulin, M. 1988, *A&A*, 190, 167
 Kifonidis, K., Plewa, T., Janka, H.-T., & Müller, E. 2003, *A&A*, 408, 621
 Langer, N., Heger, A., Woosley, S. E., & Herwig, F. 1998, in *Nuclei in the Cosmos V*, ed. N. Prantzos (Paris: Editions Frontières), 129
 Lin, Y., Gyngard, F., & Zinner, E. 2010, *ApJ*, 709, 1157
 Lodders, K. 2003, *ApJ*, 591, 1220
 Lodders, K., & Fegley, B. J. 1995, *Meteoritics*, 30, 661
 Lugaro, M., Davis, A. M., Gallino, R., et al. 2003, *ApJ*, 593, 486
 Marhas, K. K., Amari, S., Gyngard, F., Zinner, E., & Gallino, R. 2008, *ApJ*, 689, 622
 Nittler, L. R., Amari, S., Zinner, E., Woosley, S. E., & Lewis, R. S. 1996, *ApJ*, 462, L31
 Nittler, L. R., & Hoppe, P. 2005, *ApJ*, 631, L89
 Rauscher, T., Heger, A., Hoffman, R. D., & Woosley, S. E. 2002, *ApJ*, 576, 323
 Roberts, L. F., Woosley, S. E., & Hoffman, R. D. 2010, *ApJ*, 722, 954
 Tielens, A. G. G. M. 2005, *The Physics and Chemistry of the Interstellar Medium* (Cambridge: Cambridge Univ. Press)
 Timmes, F. X., Woosley, S. E., Hartmann, D. H., & Hoffman, R. D. 1996, *ApJ*, 464, 332
 Timmes, F. X., Woosley, S. E., & Weaver, T. A. 1995, *ApJS*, 98, 617
 Travaglio, C., Gallino, R., Amari, S., et al. 1999, *ApJ*, 510, 325
 Wooden, D. H., Rank, D. M., Bregman, J. D., et al. 1993, *ApJS*, 88, 477
 Woosley, S. E., Arnett, W. D., & Clayton, D. D. 1973, *ApJS*, 26, 231
 Zinner, E. 2007, in *Meteorites, Comets, and Planets*, ed. A. M. Davis (Amsterdam: Elsevier), 1
 Zinner, E., Gyngard, F., & Nittler, L. R. 2010, 41st Lunar Planet. Sci. Conf., abstract 1359